Available online at www.sciencedirect.com

ScienceDirect

Energy Procedia 78 (2015) 3234 – 3239

Energy Procedia

6th International Building Physics Conference, IBPC 2015

Characterization of the dynamic thermal properties of the opaque elements through experimental and numerical tests

G. Pernigotto[a], A. Prada[b], F. Patuzzi[b], M. Baratieri[b] and A. Gasparella[b,*]

[a]*University of Padova, Stradella San Nicola 3, Vicenza 36100, Italy*
[b]*Free University of Bozen-Bolzano, Piazza Università 5, Bolzano 39100, Italy*

Abstract

The dynamic behaviour of the building opaque elements can be characterized by the periodic thermal transmittance and the time-shift, evaluated according to EN ISO 13786:2007 prescriptions (i.e., under periodic sinusoidal forcing conditions on a side and constant conditions on the other one). A modified hotbox apparatus was built to measure these dynamic parameters. We tested a single-layer timber structure and then we developed and calibrated a numerical model with ANSYS Fluent®. Different boundary conditions have been studied in the numerical model to assess the sensitivity of the results to the boundary conditions, with the aim of refining the experimental procedure.

Peer-review under responsibility of the CENTRO CONGRESSI INTERNAZIONALE SRL
Keywords: hotbox; opaque element; periodic boundary conditions; numerical models; EN ISO 13786:2007

1. Introduction

Building energy simulation has introduced new design strategies, based on the dynamic behaviour of the building envelope, in order to improve its energy efficiency and the occupants' comfort. However, some simulation hypotheses about the elements of the opaque components (e.g., homogeneous layer with constant and isotropic thermal conductivity) can be very inaccurate for some kind of walls, for example with innovative materials, inhomogeneous layers or simply with air gaps. In these cases, experimental methods can be the most effective approach to characterize dynamic thermal behaviour, quantifiable by means of simple parameters, such as periodic

* Corresponding author. Tel.: +39 0471017200; fax: +39 0471017009.
E-mail address: andrea.gasparella@unibz.it

Peer-review under responsibility of the CENTRO CONGRESSI INTERNAZIONALE SRL
doi:10.1016/j.egypro.2015.11.786

thermal transmittance and time shift defined by EN ISO 13786:2007 [1] when constant and sinusoidal forcing temperatures are applied, respectively, to internal and external side of the wall. While for the measurement of the steady state heat transfer property, instructions are provided by technical standards such as EN 1934:1998 [2] and in the literature [3], for the evaluation of wall dynamic behaviour by means of experimental laboratory tests, there are no established references. However, some examples can be found, such as the research works by Ulgen [4], Sala *et al.* [5], Martìn *et al.* [6] and Yesilata and Turgut [7]. Moreover, a detailed evaluation of the impact of errors in imposing the boundary conditions to the specimen tested in modified hotbox apparatus is still missing. It could be challenging to get EN ISO 13786 ideal conditions, keeping the air temperature constant and realizing a sinusoidal forcing signal in practice. For this reason, as explained in previous works [8], we chose a different kind of forcing signal and used numerical techniques to extract the first harmonic, i.e., the sinusoidal signal, both for the forcing temperature and for the originated heat flux. In this research, with the support of finite volume simulation models calibrated with experimental results, we discussed the effectiveness of the implemented experimental procedure, especially as regards the imposed boundary conditions.

2. Experimental and numerical methods

2.1. Hotbox apparatus description

EN 1934:1998 was adopted as reference to design the hotbox apparatus at the Free University of Bozen-Bolzano, Italy. It consists of two boxes (height/width: 1.7 m; length: 1.1 m) made by aluminium plates with 0.1 m of polyurethane insulation (PUR). A square wall specimen (side: 1.50 m) is positioned between them. In each box, a black screen (thickness: 0.015 m) - installed to prevent radiative heat exchange between the sample and the box's walls, delimits an air gap zone of 0.039 m adjacent to the test wall. Moreover, an airflow stream is generated in the air gap by a cylindrical horizontal fan positioned on the bottom, in order to reduce vertical air temperature stratification. Each box is equipped with a cooling unit (an evaporator) and a heating unit (an electrical resistance), controlled by a PID control unit with an accuracy of ± 0.1 K in steady state conditions. For the measurement of the wall thermal conductance in steady state tests, both chambers are kept at constant temperature, respectively 20 °C and -10 °C. The thermal flux is measured on a central square section (0.5 m by 0.5 m).

For dynamic tests, only one chamber is used to maintain steady state conditions on a side of the specimen (i.e., the internal side), while a copper coil electrical heater (sizes: 1.2 m by 1.2 m; nominal thermal power: 1500 W), positioned very close to the external side, imposes the periodic forcing temperature (Fig. 1a). The heat flow variations on the internal side are measured with a heat flow meter, *HFM*, i.e., a thermopile with 250 type T thermocouples on an area of 0.5 m by 0.5 m. It consists of a rubber layer (thickness: 0.0105 m) between two layers of aluminium (thickness: 0.001 m), for a total mass of 2.3 kg. A guard ring surrounds the *HFM* and it has a thermal conductivity similar to that of the heat flow meter, which is 0.1905 W m^{-1} K^{-1} according to its calibration performed according to EN 1934:1998. Type T thermocouples connected with a reference junction compensation are used for temperature measurements due to the fast response time. 8 and 4 type T thermocouples measure the temperatures of the wall surface in thermal contact with the guard ring and the *HFM*, respectively. According to the same scheme, 12 thermocouples are positioned on the external side 0.001 m under the surface of the specimen to avoid the influence of direct irradiation from the electrical heater. A digital multimeter recorded the voltage output signal of the thermocouples and heat flow meter every 60 seconds in order to better characterize the dynamic response of the specimen.

2.2. Experimental procedure for the evaluation of dynamic parameters and tested specimen

In the dynamic tests described in this research, the internal side temperature was kept at the constant value of 23 °C to minimize the heat exchanges with the environment. The airflow rate was set to 1.5 m s^{-1} and the relative humidity was not controlled. The dynamic test started after steady state conditions were reached (i.e., 24 h). Then, the external side was exposed to 10 cycles of thermal irradiation of 1500 W for 2 h followed by 22 h of rest. This was necessary both to minimize the influence of the initial conditions and to achieve steady periodic conditions. For the analysed specimen, the transient effects were negligible after a couple of days but usually 3 or 4 days are

required. Once the amplitude of the thermal flux is constant between two periods, the steady periodic state is reached. Then, the heat flux on the internal side and the external surface temperatures are recorded.

The Fast Fourier Transform (*FFT*) algorithm [9] was implemented to compute per each day the first 720 harmonics of experimental temperatures and heat flux recorded with a sampling time of 60 s. With the first term of the Fourier approximation, the periodic thermal transmittance and the time shift are calculated. The estimated quantity is a periodic thermal transmittance without the effects of surface resistances, since surface heat fluxes and temperatures are used in calculations. The periodic thermal transmittance Y_{ie} is computed as the ratio between the amplitude of the first harmonic of two signals, the internal heat flux $\phi_{i,1}$ and the external surface temperature $\theta_{e,1}$. The time shift Δt_{ie} is calculated as the difference between the phase displacements (respectively, φ for the external surface temperature and ψ for the internal heat flux) of the first harmonics. Y_{ie} and Δt_{ie} are determined for each day of the series of recorded data in the periodic steady state condition. From the sample of daily dynamic parameters, mean values and standard deviations are calculated and provided. For this analysis, we selected as specimen a single-layer wall of massive timber with a thickness of 0.24 m. The material thermal properties were unknown. From steady state and dynamic tests, we found C_s = 0.475 W m^{-2} K^{-1}, Y_{ie} = 0.130 ± 0.07 W m^{-2} K^{-1} and Δt_{ie} = 11.64 ± 0.29 h.

2.3. Numerical simulation models: definition and calibration target

The numerical model simulates the specimen behavior in the modified hotbox apparatus under dynamic test conditions. Once chosen a proper abstraction level, it was calibrated through the characterization of the unknown material properties, considering a tolerance of 5 % with respect to the measured EN ISO 13786:2007 dynamic parameters. Moreover, the first harmonic signals from numerical results were calculated as well to be compared to the experimental ones. ANSYS Fluent® finite volume approach with conjugated heat transfer modelling between solid and fluid regions and surface-to-surface model for radiative heat exchanges was chosen. Since the fan operates at constant velocity and there is low turbulence in the air gap adjacent to the specimen, Fluent DNS was used for the flow model. After some preliminary tests to balance numerical errors and computational costs, we chose a mesh with more than 21000 quadrilateral cells, a time-discretization of 60 s which is the same time between two consecutive measurements in the experiments, a convergence criteria of $\varepsilon = 10^{-8}$ and the double precision solver.

2.4. Numerical simulation models: geometry, boundary conditions and material properties

The hotbox facility is well insulated and, in particular, the heat flows through the lateral sides of the specimen, because of its surrounding 20 cm of EPS and the additional 10 cm of sheep wool, are negligible. This allowed us to consider a 2D approach and to impose adiabatic boundary conditions on the top and the bottom sides of the specimen and of other solid regions. In order to delimit the thermo-dynamic system, we focused on the specimen and its adjacent zones on the internal side. The external wall surface was considered a solid domain boundary with the measured surface average temperature as boundary condition. As regards the vertical length of the domain, we selected the same length of the heater (i.e., 1.2 m). Border effects on top, bottom and lateral sides of the heater were expected to be negligible, especially with respect to the monitored heat flux where the *HFM* is installed (i.e., centered with respect to the electrical heater). On the internal side, all layers between the specimen surface and the black screen were included. The air gap was modelled as a fluid domain, its inlet as a velocity inlet boundary with the measured temperature of the incoming air used as input and its outlet as an outflow condition. Also in this case, border effects were assumed not significant since top and bottom sides of the measurement area are 0.36 m far from air inlet and outlet, respectively. The black screen is a solid domain and allows taking into account for the radiative exchanges on the internal side. The time-averaged measured temperature of the chamber internal air (i.e., 23.7 °C) was imposed on the side faced towards the rest of the chamber. As regards *HFM* and its guard ring, no contact resistances between them and with the internal side of the specimen were assumed.

Some material properties were unknown but only those that have a significant impact on the dynamic parameters of the specimen were chosen for calibration. Constant properties were considered and temperature-dependencies – which could be relevant especially for the specimen, were left for further developments supported by additional experimental tests. As far as the specimen is regarded, from the experimental thermal conductance, a thermal

conductivity of 0.114 W m^{-1} K^{-1} was determined. Once defined the thermal conductivity, the specific heat capacity and the density were varied in ranges admissible for timber structures, i.e., respectively, from 1000 to 2000 J kg^{-1} K^{-1} and from 300 to 400 kg m^{-3}, starting from the lower values. A thermal diffusivity of $1.781 \cdot 10^{-7}$ m^2 s^{-1} was compatible with our target of 5 % error in the estimation of Y_{ie} and Δt_{ie}. The black screen is in plywood and has a unitary surface emissivity. The same first-run properties of the specimen were assumed but, because of a small difference between boundary and average air gap temperatures (i.e., 0.4 K) and a very stable black screen temperature, no further in-depth analysis was performed. An error is introduced in this way on the heat flux but it affects the mean value and not the shape and, thus, not the dynamic parameters. For the *HFM*, we used the calibration certificate to estimate the material properties: aluminium and rubber layers have thermal conductivities of 202 W m^{-1} K^{-1} and 0.16 W m^{-1} K^{-1}, specific heat capacities of 871 J kg^{-1} K^{-1} and 840 J kg^{-1} K^{-1} and densities of 2719 kg m^{-3} and 360 kg m^{-3}. For the guard ring, the same thermal conductivity was used while 1000 kg m^{-3} and 840 J kg^{-1} K^{-1} were considered for the unknown values of density and specific heat capacity in the first-runs. We observed that the penetration depths of the harmonics of the forcing solicitation were clearly influenced but this affected marginally the measurement area. For all surfaces exposed to the air gap, an emissivity of 0.9 was assumed.

2.5. Simulated cases

After the calibration, we analysed the measured temperature profiles. On the internal side, the experimental average temperature of the air gap was 23.3 °C with a standard deviation of 0.1 K and large peaks and minimums, as effect of the hotbox heating and cooling units. On the other side, the operating cycles of the electrical heater realized an external surface temperature far from being sinusoidal. First, we simulated a case – case (1), with boundary conditions according to EN ISO 13786. In case (1), we used the average air gap temperature and the sinusoidal forcing temperature characterized by amplitude and phase averaged from those of *FFT* analysis for each day of recorded data. In the next group of cases, we coupled measured and ideal conditions: in case (2.1), we imposed constant internal temperature and measured external surface temperature while in case (2.2a), measured air gap temperature and sinusoidal forcing temperature. Then, we focused on the forcing periodic conditions and developed two alternative functions – a square and a triangle wave with the first harmonic equal to the sinusoidal forcing temperature (Fig. 1b), and coupled with internal constant conditions, respectively in cases (3.1) and (3.2). The measured air gap temperature was analysed and filtered to remove first the noise – case (2.2b), and then also peaks and minimum exceeding 0.1 K from the average value – case (2.2c). Applying *FFT* analysis to the measured air gap temperature, average amplitude and phase for the first harmonic during the 10-day test period were calculated. From those parameters, internal sinusoidal and square air temperatures were estimated and coupled with sinusoidal forcing conditions, respectively for cases (4.1) and (4.2). Similarly, once doubled the amplitude of the same signals, cases (4.3) and (4.4) were run.

3. Results

Measured and numerical heat fluxes have different average values ($\Delta\varphi \approx 1$ W m^{-2}) but similar amplitudes and phases. Fig. 1c represents, for days IV and V of the data series, the measured heat flux, both the original signal and the one processed with a second order Butterworth low-pass filter, on the left vertical axis and the numerical heat flux on a right vertical axis that is shifted of 1 W m^{-2} with respect to the left one. The first harmonics from *FFT* analysis confirm the findings from the comparison of the whole heat fluxes: regarding the amplitude, the average deviation from the 3rd to the 10th day (i.e., in periodic steady conditions) is 0.02 W m^{-2} (i.e., 4 %) while for the phase the average deviation is 0.15 rad (i.e., 2.4 % of a period). The numerical average Y_{ie} and Δt_{ie}, are 0.125 ± 0.008 W m^{-2} K^{-1} and 11.07 ± 0.16 h respectively, -3.9 % and -4.9 % with respect to the experimental ones. Table 1 reports averages and standard deviations of dynamic parameters of the simulated cases, as well as the percentage deviation of Y_{ie} and the normalized deviation of Δt_{ie} on the 24 h period with respect to the calibrated case. The highest values of standard deviations are found for the calibrated model and for those models with measured boundary conditions – the cases of group (2), and they are all within 8 % of Y_{ie} value and 10 minutes with respect of Δt_{ie} value. With the exception of case (2.2a), the simulated cases have Y_{ie} larger than that from the calibrated model and most of them is around +15 %. On the contrary, except case (2.2a), Δt_{ie} are smaller: for most of them, the normalized differences are

between 2 and 3 % lower, with the largest deviation around -4.5 % for (2.2b) and (2.2c). Performing the technical standard analytical calculation with the same material properties, Y_{ie} is 0.141 W m^{-2} K^{-1} and Δt_{ie} is 10.38 h.

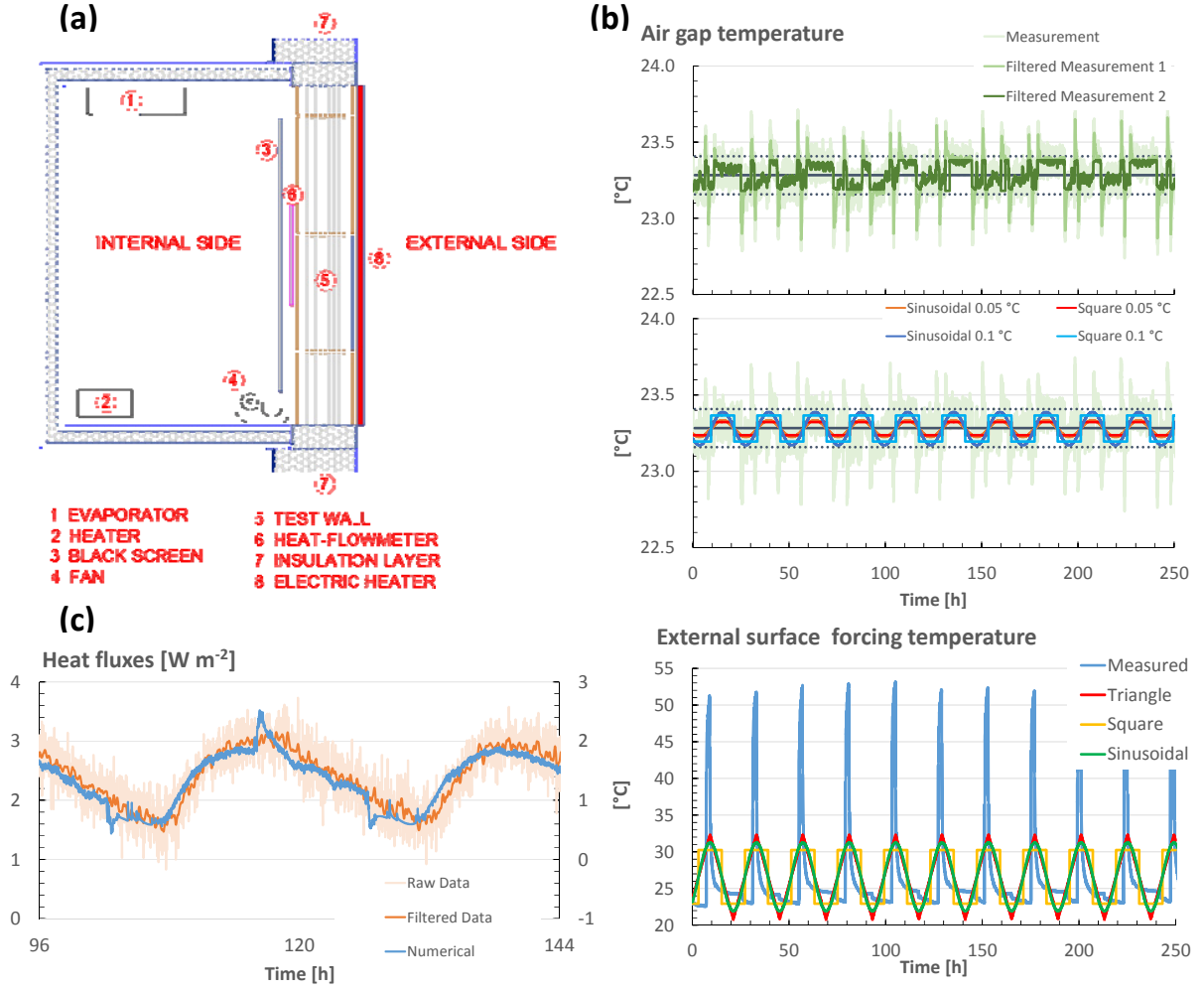

Figure 1. (a) Modified hotbox apparatus, (b) boundary conditions and (c) overlapped experimental and numerical heat fluxes for days IV and V (experimental raw and filtered data are represented on the left axis and the numerical data on the shifted right axis).

Table 1. Averages and standard deviations of dynamic parameters for simulated cases. In round brackets, the percentage deviations with respect to the results of the calibrated model

Case	Y_{ie} [W m^{-2} K^{-1}]	$\Delta(Y_{ie})$ [W m^{-2} K^{-1}]	Δt_{ie} [h]	$\Delta(\Delta t_{ie})$ [h]
Calibrated model	0.125	0.008	11.07	0.16
(1)	0.144 (*+15.2 %*)	< 0.001	10.44 (*-2.6 %*)	0.01
(2.1)	0.144 (*+15.2 %*)	0.011	10.67 (*-1.7 %*)	0.08
(2.2a)	0.110 (*-12.0 %*)	0.007	11.11 (*+0.2 %*)	0.14
(2.2b)	0.128 (*+2.4 %*)	0.007	9.98 (*-4.5 %*)	0.15
(2.2c)	0.141 (*+12.8 %*)	0.002	9.91 (*-4.8 %*)	0.06
(3.1)	0.145 (*+16.0 %*)	< 0.001	10.51 (*-2.3 %*)	0.05
(3.2)	0.142 (*+13.6 %*)	< 0.001	10.58 (*-2.0 %*)	<0.01
(4.1)	0.146 (*+16.8 %*)	0.001	10.40 (*-2.8 %*)	0.02
(4.2)	0.144 (*+15.2 %*)	0.001	10.45 (*-2.6 %*)	0.02

(4.3)	0.150 (*+20.0 %*)	< 0.001	10.30 (*-3.2 %*)	0.01
(4.4)	0.146 (*+16.8 %*)	0.001	10.44 (*-2.6 %*)	<0.01

From the cases combining measured and ideal boundary conditions, we can observe that the largest impact is due to the internal condition: indeed, while case (2.1) is pretty close to case (1), with almost the same Y_{ie} and less than 15 minutes difference for Δt_{ie}, cases (2.2) are more different. In particular, only case (2.2c), with filtered air gap temperature with respect to 0.1 K range, has both Y_{ie} close to that of case (1) and Δt_{ie} difference around 30 minutes. Changing the external surface forcing temperature does not affect significantly the results, as confirmed by cases (3.1) and (3.2), with Y_{ie} differences around 1 % with respect to case (1) and Δt_{ie} deviations of less than 10 minutes. When the internal conditions are periodic and without noise, as in cases (4), low impact is found on Y_{ie} and Δt_{ie}: the largest deviations with respect to case (1) are found for case (4.3) with a sinusoidal internal temperature of the air gap of 0.1 K of amplitude and they are +4.2 % and less than 10 minutes of Δt_{ie} underestimation.

4. Discussion and conclusions

In this work, we exploited a numerical ANSYS Fluent® model to simulate the dynamic behavior of a single layer timber wall during a dynamic test with the modified hotbox apparatus at the Free University of Bozen-Bolzano for the experimental evaluation of EN ISO 13786:2007 dynamic parameters. Once calibrated the numerical model with respect to the experimental results, we focused on the boundary conditions applied to the specimen. First, we observed that the boundary conditions imposed in the experimental activity have an impact quantified in about 15 % of underestimation of the periodic thermal transmittance and 40 minutes of overestimation of the time shift for the current specimen. However, the results are differently affected by internal and external conditions. The profile of external surface forcing temperature has little effects on the estimation of the dynamic parameter according to the proposed experimental procedure. This means that non-sinusoidal periodic forcing signals, easier to generate, can be used. On the contrary, large sensitivity was registered to the internal conditions. Non-constant but periodic internal conditions can bring results very close to those found with constant internal temperature. A good accuracy can be found also improving the control system to avoid peaks and minimum values exceeding the range of 0.1 K with respect to the average. These findings will be used as drivers for the next upgrade of the modified hotbox apparatus in order to improve the accuracy of the experimental results. Further steps of this work will focus on the heat flow meter and its response of heat flow meter in transient conditions.

References

[1] CEN. *EN ISO 13786:2007 - Thermal performance of building components - Dynamic thermal characteristics - Calculation methods*. Brussels (Belgium): CEN; 2007.
[2] CEN. *EN 1934:1998 - Thermal performance of buildings - Determination of thermal resistance by hot box method using heat flow meter*. Brussels (Belgium): CEN; 1998.
[3] Asdrubali F, Baldinelli G. Thermal Transmittance measurements with the hot box method: Calibration, experimental procedures, and uncertainty analyses of three different approaches. *Energy Build.* 2011; 43:1618-1626.
[4] Ulgen K. Experimental and theoretical investigation of effects of wall's thermophysical properties on time lag and decrement factor. *Energy Build.* 2002; 34:273-278.
[5] Sala JM, Urresti A, Martìn K, Flores I, Apaolaza A. Static and dynamic thermal characterisation of a hollow brick wall: Tests and numerical analysis. *Energy Build.* 2008; 40:1513-1520.
[6] Martìn K, Flores I, Escudero C, Apaolaza A, Sala JM. Methodology for the calculation of response factors through experimental tests and validation with simulation. *Energy Build.* 2010; 42:461–467.
[7] Yesilata B, Turgut P. A simple dynamic measurement technique for comparing thermal insulation performances of anisotropic building materials. *Energy Build.* 2007; 39:1027–1034.
[8] Pernigotto G, Prada A, Patuzzi F, Baratieri M, Gasparella A. Experimental characterization of the dynamic thermal properties of opaque elements under dynamic periodic solicitation. *Proc. Of BSA 2015 – 2nd IBPSA-Italy Conference*, Bolzano, Italy.
[9] Press WH, Teukolsky SA, Vetterling WT, Flannery BP. *Numerical Recipes: The Art of Scientific Computing*. 3rd ed. Cambridge (UK): Cambridge University Press; 2007.